63-4-1

AFCRL-62-1122

SEL-63-041

Detection of Solar Particle Streams Using High-Frequency Radio Waves

by

B. B. Lusignan

April 1963

Technical Report No. 1403-3

Prepared under
Air Force Contract No. AF19(604)-7994
Project No. 7661, Task No. 76615

Scientific Report No. 2
for
Geophysics Research Directorate
Air Force Cambridge Research Laboratories
Office of Aerospace Research, U.S. Air Force
Bedford, Massachusetts

RADIOSCIENCE LABORATORY

STANFORD ELECTRONICS LABORATORIES

STANFORD UNIVERSITY · STANFORD, CALIFORNIA

AFCRL-62-1122

SEL-63-041

DETECTION OF SOLAR PARTICLE STREAMS USING HIGH-FREQUENCY RADIO WAVES

by

B. B. Lusignan

April 1963

Technical Report No. 1403-3

Prepared under
Air Force Contract No. AF19(604)-7994
Project No. 7661, Task No. 76615

Scientific Report No. 2

for

Geophysics Research Directorate
Air Force Cambridge Research Laboratories
Office of Aerospace Research
United States Air Force Bedford, Massachusetts

Radioscience Laboratory
Stanford Electronics Laboratories
Stanford University Stanford, California

ABSTRACT

Interactions between radiowaves and charged particles change their character when the particles have high average velocities. The nature of such interactions is investigated assuming no collisions, no external magnetic field, and low particle densities. A stream of such particles makes the medium anisotropic. As a result the medium propagates two waves of unchanging (characteristic) polarization, one linearly polarized perpendicular to the particle stream and a second at right angles to the first. Such a medium can change the polarization ellipse of a propagating wave.

The sun produces such streams radiating outward either in the form of a steady "solar wind" or in bursts associated with sun spots. Three experiments are suggested to detect the streams by measuring polarization of waves propagated through them. The least sensitive of the three, moon radar, would have measurable effects only during increased solar activity, while the other two--transmission to a deep space probe and observation of polarized cosmic noise sources--show effects even during quiet solar conditions. These sensitivities are based on observations of the proton component of the solar wind.

CONTENTS

TABLES

ILLUSTRATIONS

ACKNOWLEDGMENT

I wish to express my appreciation to Professors A. M. Peterson, R. A. Helliwell, and V. R. Eshleman for their encouragement and guidance during the course of this research. The early part of the work was supported by a Bell Telephone Laboratories Fellowship, and the latter part, including preparation of the report, was supported by the Air Force Cambridge Research Laboratories under contract AF19(604)-7994.

I. INTRODUCTION

Recent satellite and space probe measurements have confirmed the existence of a "solar wind" consisting of high-velocity particle streams radiating from the sun [Refs. 1 and 2]. Although only the proton component of the wind has been measured, some properties of the electron component can be inferred from these results. Derivations of the effects of such streams show that they can cause significant depolarization of radio waves used in radar and radio astronomy and in space exploration. In particular, moon radar, transmission to deep space probes, and measurement of polarized cosmic noise sources can be used to measure properties of the electron component of the "solar wind."

In the derivations which follow, these assumptions are made:

1. Components of particle velocity caused by the radio waves are small compared to the particles' average velocity, $v \ll V$.
2. Particle collisions are negligible.
3. The effect of particles on the propagation constant of the radio wave is of second order only.
4. The effects of any external magnetic field are negligible.

Assumption 3 is not necessary to the general solution but is justified in the applications made and is therefore used for simplification. All these assumptions will be justified when specific applications are made.

There are three main effects which must be considered when particles have a high average speed. Acceleration of the particle by the magnetic field of the radio wave is no longer small compared with acceleration by the electric field of the wave. Movement of the particle relative to the radio wave causes a "doppler shift" of the fields seen by the particle. And finally the relativistic mass-momentum effects cause coupling between forces and accelerations in different coordinate directions.

This third effect enters in the particle's resistance to an accelerating force, the time derivative of the momentum,

$$\frac{d}{dt}\,(m\,\bar{v}) = \frac{d}{dt}\left[\frac{m_o\,(\bar{V}+\bar{v})}{\sqrt{1-(\bar{V}+\bar{v})\cdot(\bar{V}+\bar{v})/c^2}}\right]$$

Here the particle's velocity v is separated into a large constant component $\bar{V}$, and a small perturbation $\bar{v}$, due to the radio wave. Using small difference approximations (see Appendix A), we obtain

$$\frac{d}{dt}\left[m_o\gamma\ (\bar{V}+\bar{v})\left(1 + \frac{\gamma^2\ (\bar{v}\cdot\bar{V})}{c^2}\right)\right]$$

where

$$\gamma \triangleq \frac{1}{\sqrt{1-\beta^2}};\ \beta \triangleq \frac{V}{c}$$

Carrying out the multiplication and differentiation and once more using the inequality $v << V$, we obtain

$$m_o\gamma\ \frac{d}{dt}\left[\ \bar{v} + \frac{\gamma^2}{c^2}\bar{V}\ (\bar{v}\cdot\bar{V})\ \right]$$

For $\bar{v}$ perpendicular to $\bar{V}$ this expression is $m_o\gamma\ d(\bar{v})/dt$, but for $\bar{v}$ parallel to $\bar{V}$ it becomes $m_o\gamma(1+\gamma^2\beta^2)\ d(\bar{v})/dt$. Thus, if a particle is accelerated perpendicular to its high velocity, its effective mass is just its rest mass m_o times γ. But when it is accelerated in the same direction as its high velocity, it appears to be heavier by a fraction $\gamma^2\beta^2$ than the ordinary value γm_o.

Thus the medium is anisotropic; radio waves linearly polarized perpendicular to a stream see particles of one mass, while waves parallel to the stream see a different effective mass. If the stream is at some angle other than 90° to the propagation direction of the wave, the interactions are more complex. However, for velocities much less than relativistic, this effect as described is sufficient to account for the results if the quantity $\gamma^2\beta^2$ is replaced by $\gamma^2\beta^2\cos^2\theta$, where θ is the angle between the radio wave's ray and the particle velocity.

II. DERIVATIONS

A. METHOD OF SOLUTION

In solving the interaction problem, first the high-velocity motion of the particle is described mathematically. The radio wave, assumed to vary as $\exp j(\omega t - x)$, is then added to the particle-motion equations. At this point the high-velocity effects previously described are introduced and simplifying approximations made. The resulting equations are solved for the radio-frequency particle motion in terms of the radio-wave and particle high-velocity parameters. The distribution of particle density with velocity (Boltzmann's distribution) is chosen to describe the medium being considered. The radio-frequency particle motion is averaged over this distribution to give the space current as a function of the radio-wave parameters. Finally, these results are combined with Maxwell's equations to give an expression for Γ, the propagation constant of the radio waves.

B. PARTICLE-MOTION EQUATIONS

With no radio waves or external magnetic field the particle will move in a straight line with high velocity, $\bar{V}$. A propagating radio wave causes perturbations of this velocity. In the wave's coordinates the high velocity is described by the angle θ and the magnitude V as shown in Fig. 1a. The relativistic velocity components are then:

$$V_x = V \sin \theta; \quad V_y = -V \cos \theta; \quad V_z = 0 \tag{1}$$

To simplify the equations, the y axis is chosen so that $\bar{V}$ lies in the x-y plane. The more general situation is found later by a rotation of axes as shown in Fig. 1b.

The particle velocity is perturbed by a plane EM wave of radian frequency ω propagating in the plus x direction. The space and time dependence of this wave are given by $\exp j(\omega t - \Gamma x)$, where Γ is to be determined. For such a wave, Maxwell's equations in cartesian coordinates become:

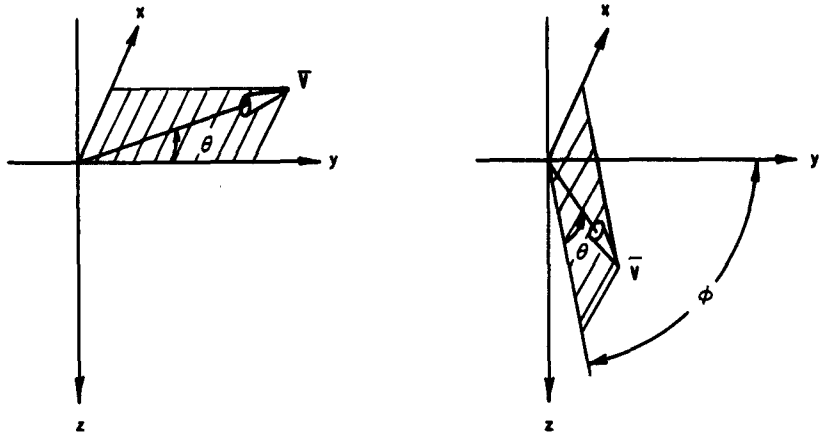

a. Particle velocity lies in x-y plane.

b. Particle velocity lies at angle ϕ from x-y plane.

FIG. 1. DEFINITION OF COORDINATES.

$$\left.\begin{aligned} E_x &= -\frac{i_x}{j\omega k_o}; & H_x &= 0 \\ E_y &= -\frac{i_y}{j\omega k_o}\left(1 - \frac{\Gamma^2}{\omega^2\mu_o k_o}\right); & H_y &= -\left(\frac{\Gamma}{\omega\mu_o}\right)E_z \\ E_z &= -\frac{i_z}{j\omega k_o}\left(1 - \frac{\Gamma^2}{\omega^2\mu_o k_o}\right); & H_z &= +\left(\frac{\Gamma}{\omega\mu_o}\right)E_y \end{aligned}\right\} \qquad (2)$$

where k_o and μ_o are the dielectric constant and permeability of free space.

Currents i_x, i_y, and i_z are due to the perturbation velocities of the particles v_x, v_y, and v_z, which are found by solving the particle-motion equations:

$$\left.\begin{aligned} \frac{d[m(V_x + v_x)]}{dt} &= qE_x - q\mu_o(V_z + v_z)H_y + q\mu_o(V_y + v_y)H_z \\ \frac{d[m(V_y + v_y)]}{dt} &= qE_y - q\mu_o(V_x + v_x)H_z \\ \frac{d[m(V_z + v_z)]}{dt} &= qE_z + q\mu_o(V_x + v_x)H_y \end{aligned}\right\} \qquad (3)$$

The dc current due to $\bar{V}$ does not interact directly with the radio wave, although it may have an effect on the distribution of particle density with velocity. In the problem being considered this distribution is assumed to be given.

At this point the three high-velocity effects enter. The relativistic momentum effect can be expressed as a time variation of the mass given by:

$$m = m_o\gamma(1 + d) \tag{4}$$

where

$$d \triangleq \left(\frac{\gamma^2\beta^2}{V^2}\right)(v_xV_x + v_yV_y + v_zV_z); \quad \beta \triangleq \frac{V}{c}; \quad \gamma \triangleq (1 - \beta^2)^{-\frac{1}{2}}$$

In deriving d (Appendix A), it is assumed that $v << V$.

Time derivatives in the particle-motion equations show the second effect, the apparent doppler shift of the forcing functions (Appendix B). Such derivatives generate factors $j\omega(1 - V_x\Gamma/\omega)$ instead of $j\omega$. The third effect is the inclusion of the magnetic field terms in the equations. The terms V_xH_y, V_yH_z, etc., must be considered (v_xH_z, v_yH_z, etc., can be ignored since $v << V$). Substituting for m from (4), for H_y and H_z from (2), and for V_x, V_y, and V_z from (1), and making the indicated approximations, Eqs. (3) becomes:

$$j\omega m_o\gamma[v_x(1 + R\sin^2\theta) + v_yR\sin\theta\cos\theta]\left(1 - V\sin\frac{\theta\Gamma}{\omega}\right)$$

$$= qE_x + \left(qV\cos\frac{\theta\Gamma}{\omega}\right)E_y \tag{5}$$

$$j\omega m_o\gamma[v_y(1 + R\cos^2\theta) + v_xR\sin\theta\cos\theta] = qE_y \tag{6}$$

$$j\omega m_o\gamma[v_z] = qE_z \tag{7}$$

where $R \triangleq \beta^2/\gamma^2 = \beta^2/(1 - \beta^2)$. The factor $(1 - V\sin\theta\Gamma/\omega)$ in Eq. (5) describes the doppler shift effect. In Eqs. (6) and (7) an identical term appeared on the right due to the magnetic field effect and cancelled the doppler term. These three equations are solved to give the velocities as functions of the accelerating fields.

$$\left.\begin{aligned} v_x &= A_{11}E_x + A_{12}E_y \\ v_y &= A_{21}E_x + A_{22}E_y \\ v_z &= A_{33}E_z \end{aligned}\right\} \qquad (8)$$

where the parameters A_{ij} are defined as follows:

$$\left.\begin{aligned} A_{11} &= \frac{-jq}{\omega m_o \gamma(1+R)}\left[\frac{1+R\cos^2\theta}{1 - V\sin\theta\,\Gamma/\omega}\right] \\ A_{12} &= \frac{-jq}{\omega m_o \gamma(1+R)}\left[-R\sin\theta\cos\theta + \frac{(V\cos\theta\,\Gamma/\omega)(1+R\cos^2\theta)}{(1 - V\sin\theta\,\Gamma/\omega)}\right] \\ A_{21} &= \frac{-jq}{\omega m_o \gamma(1+R)}\left[\frac{-R\sin\theta\cos\theta}{1 - V\sin\theta\,\Gamma/\omega}\right] \\ A_{22} &= \frac{-jq}{\omega m_o \gamma(1+R)}\left[1+R\sin^2\theta - \frac{(V\cos\theta\,\Gamma/\omega)(R\sin\theta\cos\theta)}{(1 - V\sin\theta\,\Gamma/\omega)}\right] \\ A_{33} &= \frac{-jq}{\omega m_o \gamma} \end{aligned}\right\} \qquad (9)$$

If the particle velocity is at some angle ϕ with respect to the x-y plane (Fig. 1b), a simple transformation of axes gives the velocity components:

$$\left.\begin{aligned} v_x &= A_{11}E_x + A_{12}\cos\phi\,E_y + A_{12}\sin\phi\,E_z \\ v_y &= A_{21}\cos\phi\,E_x + (A_{22}\cos^2\phi + A_{33}\sin^2\phi)E_y \\ &\quad + (A_{22} - A_{33})\sin\phi\cos\phi\,E_z \\ v_z &= A_{21}\sin\phi\,E_x + (A_{22} - A_{33})\sin\phi\cos\phi\,E_y \\ &\quad + (A_{22}\sin^2\phi + A_{33}\cos^2\phi)E_z \end{aligned}\right\} \qquad (10)$$

C. EFFECTS OF PARTICLE VELOCITY DISTRIBUTION

To obtain a solution from (10) it is necessary to define a particle density function $n(V,\theta,\phi)$ describing the velocity distribution of particles (Boltzmann's function) such that

$$\iiint n(V,\theta,\phi)\ dV\ d\theta\ d\phi = N_o \quad \text{particles/m}^3 \tag{11}$$

where N_o is the average particle density. Once this distribution is defined, the currents can be expressed as:

$$\left.\begin{aligned} i_x &= B_{11}E_x + B_{12}E_y + B_{13}E_z \\ i_y &= B_{21}E_x + B_{22}E_y + B_{23}E_z \\ i_z &= B_{31}E_x + B_{32}E_y + B_{33}E_z \end{aligned}\right\} \tag{12}$$

where the quantities B_{ij} are defined as:

$$\left.\begin{aligned} B_{11} &= q \iiint A_{11}\, n\ dV\ d\theta\ d\phi \\ B_{12} &= q \iiint A_{12} \cos\phi\, n\ dV\ d\theta\ d\phi \\ B_{13} &= q \iiint A_{12} \sin\phi\, n\ dV\ d\theta\ d\phi \\ B_{21} &= q \iiint A_{21} \cos\phi\, n\ dV\ d\theta\ d\phi \\ B_{22} &= q \iiint (A_{22}\cos^2\phi + A_{33}\sin^2\phi)\, n\ dV\ d\theta\ d\phi \\ B_{23} &= q \iiint (A_{22} - A_{33}) \sin\phi\cos\phi\, n\ dV\ d\theta\ d\phi \\ B_{31} &= q \iiint A_{21} \sin\phi\, n\ dV\ d\theta\ d\phi \\ B_{32} &= q \iiint (A_{22} - A_{33}) \sin\phi\cos\phi\, n\ dV\ d\theta\ d\phi \\ B_{33} &= q \iiint (A_{22}\sin^2\phi + A_{33}\cos^2\phi)\, n\ dV\ d\theta\ d\phi \end{aligned}\right\} \tag{13}$$

For a random distribution of particle directions the particle density function can be expressed as:

$$n(V,\theta,\phi) = \left(\frac{N_o}{4\pi^2}\right) n(V); \qquad \int^{V} n(V)\ dV = 1.$$

When this expression is substituted into the expressions for B_{ij}, all but three coefficients go to zero. Those remaining are

$$B_{11} = -\frac{jq^2N_o}{\omega m_o}\int^V \frac{\eta(V)}{\gamma(1+R)}\left[\frac{R\omega^2}{V^2\Gamma^2} + \frac{1+R(1-\omega^2/V^2\Gamma^2)}{\sqrt{1-V^2\Gamma^2/\omega^2}}\right] dV$$

$$B_{22} = B_{33} = -\frac{jq^2N_o}{\omega m_o}\int^V \frac{\eta(V)}{\gamma(1+R)}\left[1 + \frac{R\omega^2}{2V^2\Gamma^2}\left(1 - \sqrt{1-\frac{V^2\Gamma^2}{\omega^2}}\right)\right] dV$$

In applications where particle densities are large enough to cause first-order changes in Γ, these expressions, when combined with Maxwell's equations, may yield some interesting results. However, for low particle densities, the quantity $V\Gamma/\omega$ can be replaced by β in the above expressions since $\Gamma/\omega = 1/c$ to the first order. The expression for Γ then becomes:

$$\Gamma = \frac{\omega}{c}\sqrt{1+\frac{B_{22}}{j\omega k_o}} = \frac{\omega}{c}\sqrt{1-\frac{q^2N_R}{\omega^2 m_o k_o}} \qquad (15)$$

$$N_R \triangleq N_o \int^V \frac{\eta(V)}{\gamma}\left(\frac{3}{2} - \beta^2 - \frac{1}{2}\sqrt{1-\beta^2}\right) dV.$$

This result is the same as that for low-velocity particles except that the effective density N_R is lower than the actual density N_o. It would therefore be very difficult to distinguish the effects of high-velocity and low-velocity particles when both are present.

For a stream of particles all having the same direction, the results are more encouraging. The particle-density function for this case can be expressed as:

$$\eta(V,\theta,\phi) = N_o\delta(\Theta,0)\eta(V)$$

where $\delta(\Theta,0)$ is the two-dimensional Dirac delta function, defined by $\int F(\theta,\phi)\ \delta(\Theta,0)\ d\theta\ d\phi = F(\Theta,0)$.

The direction of the stream has been chosen to lie in the x-y plane, $\phi = 0$, making an angle $\theta = \Theta$ with the y axis. Now only four of the nine coefficients, B_{ij}, are zero. Thos remaining are:

$$
\left.
\begin{aligned}
B_{11} &= \frac{-jqN_o}{\omega m_o} \int^V \frac{\eta(V)(1 + R\cos^2\theta)}{\gamma(1+R)(1 - [V\Gamma/\omega]\sin\theta)}\, dV \\
B_{12} &= \frac{-jqN_o}{\omega m_o} \int^V \frac{\eta(V)}{\gamma(1+R)} \left[-R\sin\theta\cos\theta \right. \\
&\qquad \left. + \frac{(V\Gamma/\omega)\cos\theta\,(1 + R\cos^2\theta)}{(1 - [V\Gamma/\omega]\sin\theta)} \right] dV \\
B_{21} &= \frac{+jqN_o}{\omega m_o} \int^V \frac{\eta(V) R\sin\theta\cos\theta\, dV}{\gamma(1+R)(1 - [V\Gamma/\omega]\sin\theta)} \\
B_{22} &= \frac{-jqN_o}{\omega m_o} \int^V \frac{\eta(V)}{\gamma(1+R)} \left[1 + R\sin^2\theta \right. \\
&\qquad \left. - \frac{(V\Gamma/\omega) R\sin\theta\cos\theta}{(1 - [V\Gamma/\omega]\sin\theta)} \right] dV \\
B_{33} &= \frac{-jqN_o}{\omega m_o} \int^V \frac{\eta(V)}{\gamma}\, dV
\end{aligned}
\right\} \qquad (16)
$$

Maxwell's equations, (2), now become:

$$
\left.
\begin{aligned}
E_x &= -\left(\frac{B_{11}}{j\omega k_o}\right) E_x - \left(\frac{B_{12}}{j\omega k_o}\right) E_y \\
E_y &= \frac{-(B_{21}/j\omega k_o)\, E_x - (B_{22}/j\omega k_o)\, E_y}{1 - (\Gamma^2/\omega^2\mu_o k_o)} \\
E_z &= \frac{-(B_{33}/j\omega k_o)\, E_z}{1 - (\Gamma^2/\omega^2\mu_o k_o)}
\end{aligned}
\right\} \qquad (17)
$$

The third equation involves only E_z and Γ, indicating that this wave (the one with its E field in the z direction, i.e., perpendicular to the stream flow) is a characteristic wave of the medium. It will

travel unchanged through the medium with propagation constant, Γ_o, given by

$$\Gamma_o = \frac{\omega}{c}\sqrt{1 + \frac{B_{33}}{j\omega k_o}} = \frac{\omega}{c}\sqrt{1 - \frac{q^2 N_{Ro}}{\omega^2 m_o k_o}} \tag{18}$$

where

$$N_{Ro} \triangleq N_o \int^V \frac{\eta(V)}{\gamma}\, dV$$

This propagation constant is identical to that for low-energy particles except for the relativistic mass correction, $1/\gamma$. Therefore this wave will be called the "ordinary" wave.

The second characteristic wave of the medium has its E field polarized primarily in the y direction, with some E field in the x direction, the direction of propagation. The ratio between these two components is given by

$$\frac{E_x}{E_y} = \frac{(-B_{12}/j\omega k_o)}{1 + (B_{11}/j\omega k_o)}$$

which is much less than one for low particle densities. This "extraordinary" wave has propagation constant, Γ_x, found from (17) to be:

$$\Gamma_x = \frac{\omega}{c}\sqrt{1 + \frac{B_{22}}{j\omega k_o} - \frac{(B_{12}/j\omega k_o)(B_{21}/j\omega k_o)}{1 + (B_{11}/j\omega k_o)}} \tag{19}$$

From (16) it is apparent that all terms, $B_{ij}/j\omega k_o$, are of the order of $(q^2 N_o/\omega^2 m_o k_o)$, which for low particle densities is $\ll 1$. For this reason in (19) the term involving B_{12}, B_{21}, and B_{11} can be ignored with respect to B_{22}; and in B_{22} the quantity β can be substituted for $(V\Gamma/\omega)$ as before. The expression then becomes:

$$\Gamma_x = \frac{\omega}{c}\sqrt{1 + \frac{B_{22}}{j\omega k_o}} = \frac{\omega}{c}\sqrt{1 - \frac{q^2 N_{RX}}{\omega^2 m_o k_o}} \tag{20}$$

where

$$N_{RX} = N_o \int^{V} \frac{\eta(V)}{\gamma(1+R)} \left[1 + R^2 \sin^2 \theta - \frac{2R \sin \theta \cos \theta}{1 - \beta \sin \theta} \right] dV$$

Thus, a medium containing a low-density, high-energy particle stream splits a wave into two linearly polarized characteristic waves. The "ordinary" wave, polarized perpendicular to the particle stream, has a propagation constant Γ_o; and the "extraordinary" wave, at right angles to the first, has a propagation constant Γ_x.

Before applying these results, more general particle distributions will be considered. Since the coefficients B_{ij} are found by summing (integrating) the effects of individual particles, the coefficients for a medium containing two distributions of particles are the sums of the coefficients for each distribution. Thus the B_{ij} for a stream passing through a random distribution would be found by adding appropriate amounts of the coefficients from (14) and (16).

For such a distribution the coefficients, B_{13}, B_{23}, B_{31}, and B_{32}, are zero as before. In fact, (13) shows these to be zero for any $\eta(V,\theta,\phi)$ that is an even function of ϕ. The characteristic waves of such a medium will therefore be the same as for a pure stream and the propagation constants will be given by (18) and (19). The only change is that the effective densities, N_{Ro} and N_{RX}, will be given by the B_{33} and B_{22} appropriate to the new particle distribution. Thus, to get the two linearly polarized characteristic waves it is not necessary to have a pure particle stream but only a net particle flow in some direction.

D. EFFECTS OF PARTICLE-STREAM PARAMETERS

The effects of a high-velocity particle stream on a radio wave have been described in terms of two characteristic waves, with propagation constants Γ_o and Γ_x. They will now be analyzed in terms of the phase path difference between the characteristic waves of the medium; and the effects of the particles' direction, energy, and density will be described. Although all that follows is based on the results for a pure stream (all particles traveling in exactly the same direction), it is applicable to divergent streams with only slight modification as described above.

Any wave entering a medium containing a high-energy stream will split into the two characteristic waves. They will traverse the medium and emerge with phase changes given by:

$$\theta_o = \Gamma_o D; \text{ and } \theta_x = \Gamma_x D$$

where D is the distance across the medium. Since Γ_o and Γ_x are different, the two emerging waves will have shifted their relative time phases. This change is given by (18) and (20).

$$\phi_p = \theta_o - \theta_x = D(\Gamma_o - \Gamma_x) = D\left(\frac{\omega}{c}\right)\left(\sqrt{1 - \frac{q^2 N_{Ro}}{\omega^2 m_o k_o}} - \sqrt{1 - \frac{q^2 N_{RX}}{\omega^2 m_o k_o}}\right)$$

Assuming again very low density $(q^2N_o^2/\omega^2 m_o k_o << 1)$, this simplifies to:

$$\phi_p = -D\left(\frac{\omega}{c}\right)\left(\frac{\omega_o^2}{\omega^2}\right)\frac{1}{2}\int^V \eta(V)\,\Delta(V)\,dV \qquad (22)$$

where $\omega_o^2 \triangleq q^2 N_o / m_o k_o$; and

$$\Delta(V) = \frac{1}{\gamma}\left[\beta^2 \cos^2\Theta + \frac{\beta^3 \sin\Theta \cos\Theta}{(1 - \beta \sin\Theta)}\right] \qquad (23)$$

To determine what energy range of particles contributes most to the relative phase shift, the variation of $\Delta(V)$ with energy at $\Theta = 0^o$ is considered.

$$\Delta(V)_{\Theta=0^o} = \frac{\beta^2}{\gamma} = \beta^2\sqrt{1 - \beta^2}$$

The dependence of this function on β is shown in Fig. 2. Both β and the equivalent total electron energy are shown. As particle speed increases, the high-velocity effects gain in importance relative to the normal effects. However, as the speed increases the effective mass of the particles, γm_o, also increases, making them less sensitive to the radio wave. Thus as $\beta \to 1$, the relative effects of high energy continue to increase, but the total effect of the particles decreases. The value of Δ reaches a peak near $\beta = 0.8$, and then decreases for $\beta > 0.8$. At lower velocities the effects decrease as β^2.

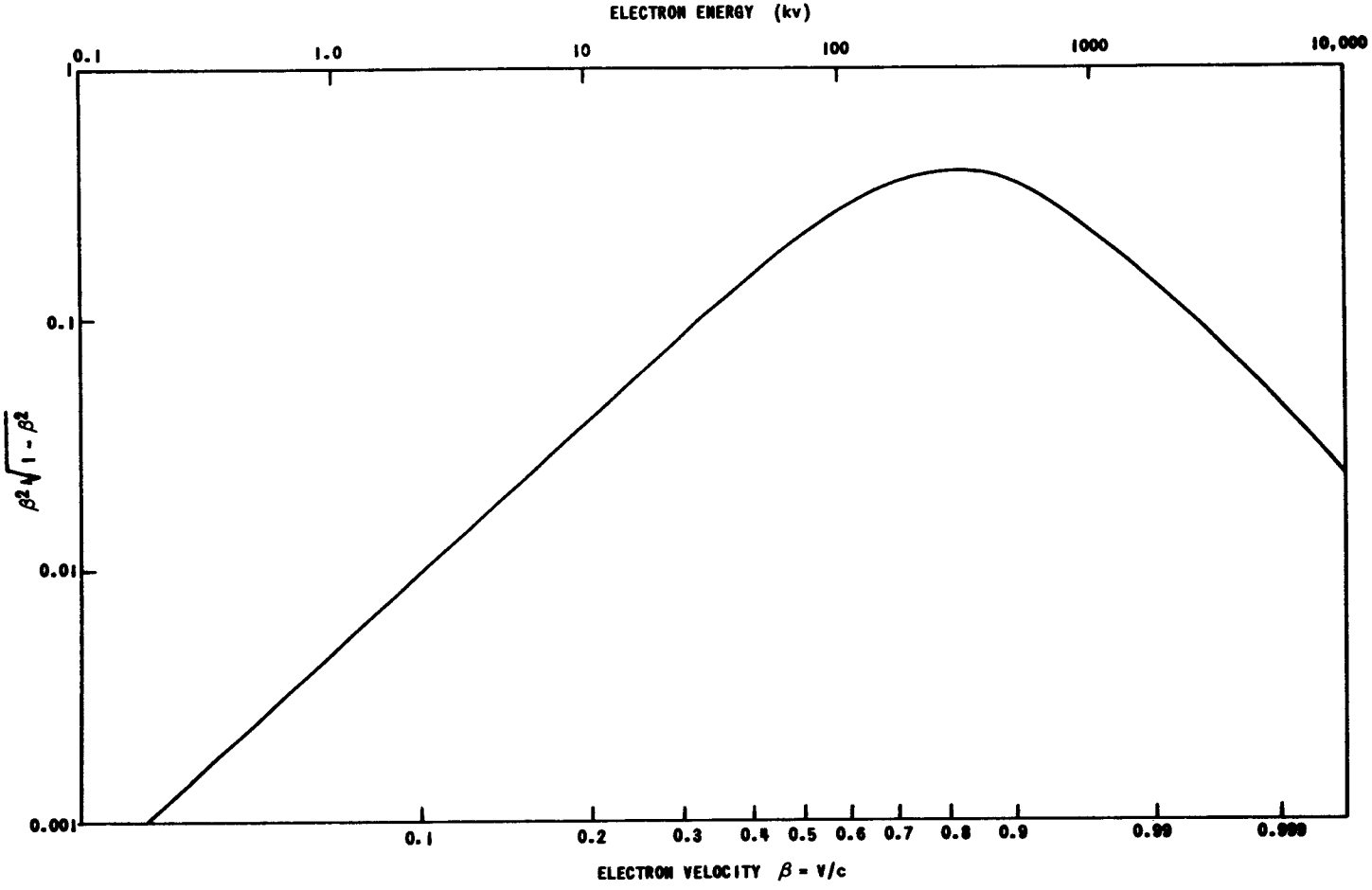

FIG. 2. PHASE SHIFT VS STREAM VELOCITY. Phase shift dependence, $\beta^2\sqrt{1-\beta^2}$, is plotted as a function of β. The equivalent electron energy is also shown.

In Fig. 3 the complete dependence of Δ on θ and β is plotted. This shows that the phase change will be zero when $\theta = \pm 90^{\circ}$, i.e., when the particle stream is parallel with the wave normal. At this point both "ordinary" and "extraordinary" waves have their E fields perpendicular to the particle stream and have identical interactions with the particles, with the result that $\Gamma_o = \Gamma_x$. The angle corresponding to maximum Δ depends on β. For very small β it is near 0° and swings toward $+90^{\circ}$ as β approaches 1. Also shown in Fig. 3 is

$$\frac{1}{2}\left[\Delta(\theta) + \Delta(-\theta)\right]$$

which indicates the average effect on a wave passing and returning through the medium, as in a moon-radar experiment.

The particle density necessary to give measurable effects depends on the dimension of the particle stream D, the particles' velocity β, and the frequency of the radio wave ω, according to Eq. (22). This dependence is shown in Fig. 4, assuming that a phase change of $\phi_p \approx 10^{\circ}$ is detectable. The electron density N_o is shown calibrated for three different particle velocities, $\beta = 0.7$, 0.085, and 0.002. The necessary proton density would be this electron density multiplied by 1838, the ratio of proton to electron mass.

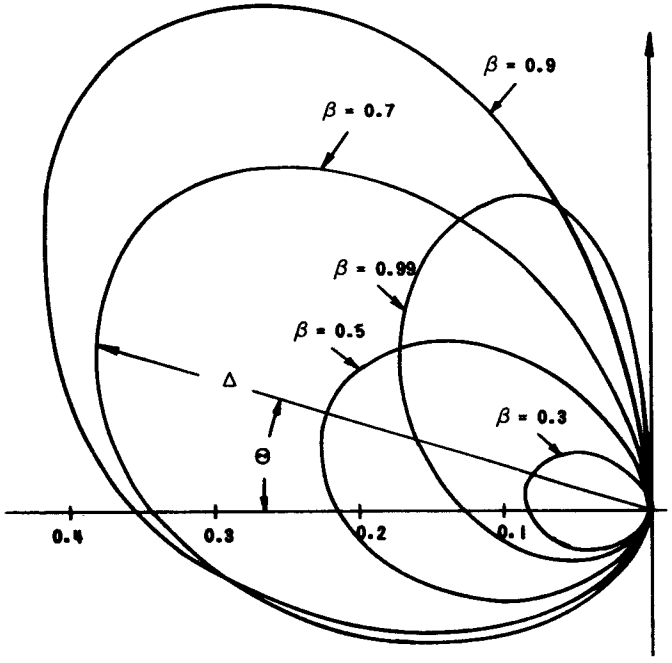

a. Differential phase shift, Δ, is shown as a function of β and Θ.

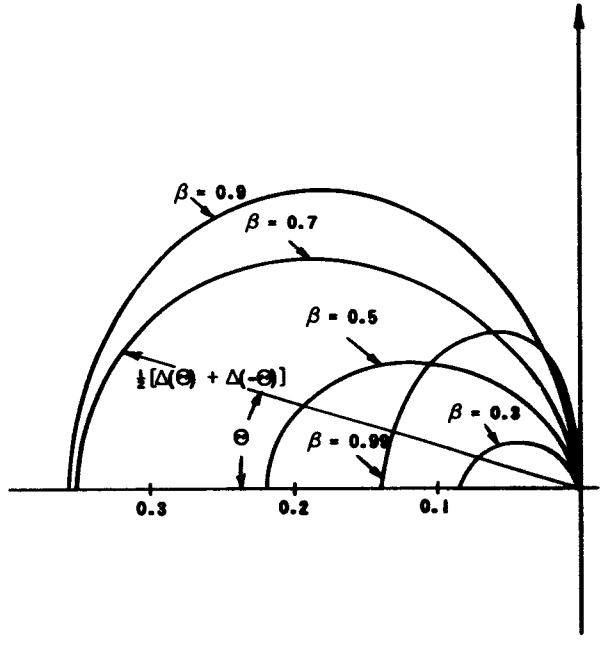

b. Δ is averaged for $\Theta+$ and $\Theta-$ to show total dependence on a two-way radar path.

FIG. 3. PHASE SHIFT VS STREAM VELOCITY AND DIRECTION.

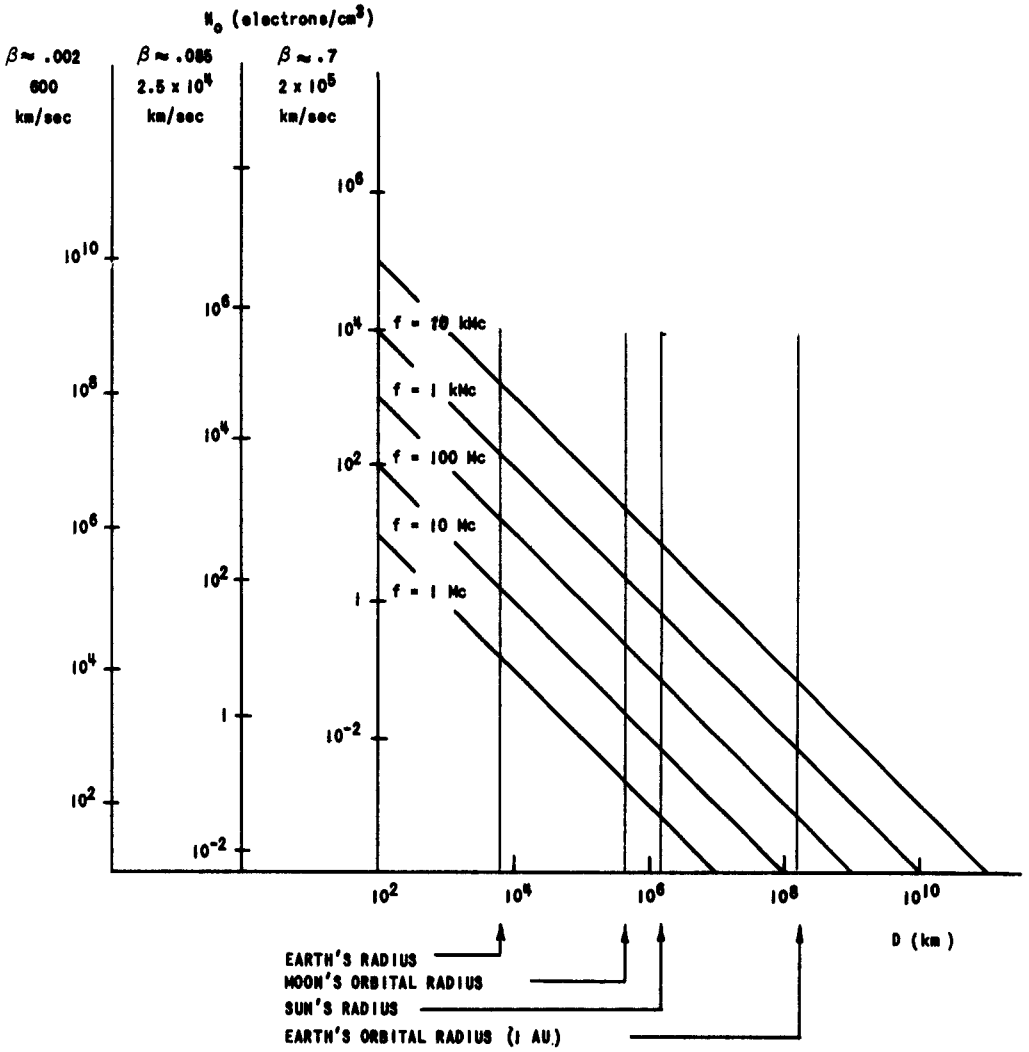

FIG. 4. PHASE SHIFT VS FREQUENCY, DENSITY, AND VELOCITY. The stream density, N_o required to give 10^o phase shift is shown as a function of distance D for various frequencies f. The densities are shown for three particle velocities, $\beta = V/c$.

III. EXPERIMENTAL APPLICATIONS

A. SOLAR PARTICLE STREAMS

The previous calculations show that radio waves can be used to detect the "solar wind" or particle bursts associated with solar flares. The radio frequency and distance required for detection depend on the expected particle velocities and densities, which have been measured directly by satellites and deep space probes for the proton component of the wind. It normally contains about 5 protons/cm^3 (at the earth), moving radially from the sun at speeds of about 600 km/sec. These quantities vary with time, and during increased solar activity can rise to speeds of 1500 km/sec and densities of 100 protons/cm^3 [Refs. 1 and 2]. However, because of their much greater mass, the protons affect the radio wave much less than do the electrons.

Although the electron component has not been directly measured, some of its properties can be inferred from the proton component. Both charge neutrality on the sun and the lack of strong magnetic fields in space imply an approximate balance between electron and proton currents, which requires that

$$N_o = N_p(\beta_p/\beta)$$

N_o and N_p are the equivalent electron and proton stream densities, in particles/cm^3, and β and β_p are the mean electron and proton speeds. The equivalent particle densities are defined so that $N_o\beta$ and $N_p\beta_p$ are equal to the electron and proton current densities. This implies that if the *total* densities are the same and the electrons have greater velocity, they must necessarily have a more random distribution so that the stream density is lower and thus the electron current (density multiplied by velocity) is equal to the proton current.

To determine N_o, then, an estimate of the electron speed β must be made. A reasonable lower limit is obtained by assuming electron and proton speeds equal, $\beta = \beta_p$, $N_o = N_p$; and a reasonable upper limit is obtained by assuming electron and proton energies equal,

$$\beta = \beta_p\sqrt{m_p/m_e}, \quad N_o = N_p/\sqrt{m_p/m_e}$$

where m_p and m_e are the masses of the proton and electron respectively. Note that since the stream effects are proportional to $N_o\beta^2$ and N_o is proportional to $1/\beta$ for a given proton stream, the stream effects

increase directly with β, i.e., the higher electron energy is more favorable to detection. The limits of N_o and β are shown in Table 1 for both quiet and disturbed solar conditions. Values are based on measurements of solar-wind proton streams.

TABLE 1. DENSITIES OF SOLAR-WIND ELECTRON STREAMS

Solar Condition	Minimum		Maximum	
	$\beta = \frac{V}{c}$	N_o	$\beta = \frac{V}{c}$	N_o
Quiet sun	0.002	$5/cm^3$	0.085	$0.12/cm^3$
Disturbed sun	0.005	$100/cm^3$	0.21	$2.3/cm^3$

B. JUSTIFICATION OF ASSUMPTIONS

In the three experiments to be described, interaction of the radio wave with the solar particle stream takes place in outer space where chances of particle collisions are very small due to the extremely low densities (Assumption 2, Chapter I). These low densities also insure that at the frequencies used, all greater than 20 Mc, the effect of the particles on the propagation constant of the wave will be of second order (Assumption 4). In fact they are so small that many thousands of wavelengths are needed to accumulate measurable effects.

Assumption 1, $v >> V$, is easily checked by calculating the approximate field strength of a radio wave required to give a maximum velocity v_{max} equal to the minimum stream velocity, approximately 300 km/sec. This field strength, E_{req}, is given by

$$E_{req} = \frac{v_{max}\, \omega m}{q}$$

which for $v_{max} = 300$ km/sec at $f = 20$ Mc has a value of about 2 v/cm. Since the transmitters in the experiments, either earthbound radar or cosmic noise sources, cannot develop fields in space anywhere near this strength, the assumption is verified.

Finally, Assumption 3 states that there is no appreciable external magnetic field in the plasma. Quantitatively this requires that forces on the particle due to the product of its steady velocity times the wave's magnetic field are much greater than those due to the varying component

of its velocity times the external field. When this is expressed algebraically it is found to be equivalent to

$$\frac{1}{2\pi}\frac{\text{(wavelength of the radio wave)}}{\text{(gyro radius of the particle)}} \ll 1$$

For a velocity of 300 km/sec and a frequency of 20 Mc this ratio is less than 0.1 for magnetic fields below 70γ, which corresponds to an electron gyro frequency of 2 kc. Since space-probe measurements find normal values of 5 to 10γ, rising to about 50γ during increased solar activity, it is safe to ignore the magnetic field in interplanetary space.

Within the earth's magnetosphere, however, the inequality is no longer true and the external magnetic field must be considered. In fact, below an altitude of 7,000 km (about one earth radius) this ratio is greater than 10 and only the magnetoionic effects need be considered. But from here out to 10 earth radii both effects must be considered. (Beyond this the earth's field is less than 70γ.) This region contains both low-energy electrons in the upper extension of the ionosphere and high-energy electrons trapped in the Van Allen belts.

The spiral motion of the particles in the magnetic field adds a sinusoidally varying component to the steady component of the high-velocity particle motion, which must be included in addition to the product of the magnetic field and rf velocity in the equations. This also means that in the particle reference frame the fields of the radio wave appear to be phase modulated at the gyro frequency. These effects add sidebands to the rf particle motion at multiples of the gyro frequency. The resulting equations can be transformed to a set of difference equations and solved using an electronic computer. A program has been written to do this and enough runs made to determine that the effects, although different in character, are of the same order of magnitude as the effects in the absence of the field and depend on the particle density and energy, radio frequency, and distance in the same way.

For particle energies above about 40 kev, $\beta = 0.4$ and greater, Fig. 4 indicates that a density of near 0.5/cm^3 would be needed to give measurable effects over 10 earth radii at 20 Mc. This corresponds to a particle flux of about 10^9/cm^{2}sec. Recent satellite measurements indicate that fluxes less than 10^8/cm^{2}sec are expected at these energies [Ref. 3]. Although the spectrum at lower energies is not well known, some approximations can be made. If a density energy dependence of the form $E^{-2.5}$ is assumed, the density per unit velocity at 250 ev must be

at least 10^{-6} $cm^{-4}sec$ to have an appreciable effect. It is assumed that this dependence extends down to an energy where the total integrated density equals the total density of the region, $\approx 1000/cm^3$ at an altitude of one earth radius [Ref. 4]. Measurement of whistler attenuation indicates that values of density per unit velocity interval less than 10^{-9} $cm^{-4}sec$ exist at 250 ev [Ref. 5]. Note that the approximations made here are not intended to conform to a realistic picture of this region but rather to err only in the direction of exaggerating its effects. It is therefore obvious that the effects in the region from 1 to 10 earth radii are negligible for radio frequencies greater than 20 Mc.

C. GENERAL DESCRIPTION OF EXPERIMENTS

In the first two experiments the radio wave is transmitted from earth and passes out through the ionosphere before entering outer space. In the ionosphere it undergoes Faraday rotation, whose magnitude depends on the earth's magnetic field and particle density [Ref. 6]. It then enters outer space where it excites some of each characteristic wave in the particle stream. The two waves continue on, changing relative time phase as they go.

This process is illustrated in Fig. 5 for three different cases. Here the polarization ellipse of the total wave is shown at various stages of its journey. In (a) the transmitted wave is circularly polarized and travels through the ionosphere unchanged. It therefore excites the "O" and "X" waves in equal magnitude but 90^o out of time phase. This phase then shifts, changing the polarization from circular to elliptical, to linear, to elliptical, etc., as shown. In (b) a linearly polarized wave propagates through the ionosphere undergoing Faraday rotation. Entering space it excites unequal amounts of "O" and "X" waves which then change phase as before. Since unequal amounts of the two waves are excited, the polarization never becomes circular but rather changes back and forth between linear and elliptical. In the third illustration, (c), the Faraday rotation and initial linear polarization are such as to excite only one of the characteristic waves, in this case the "X" mode. The wave therefore maintains this polarization as it propagates.

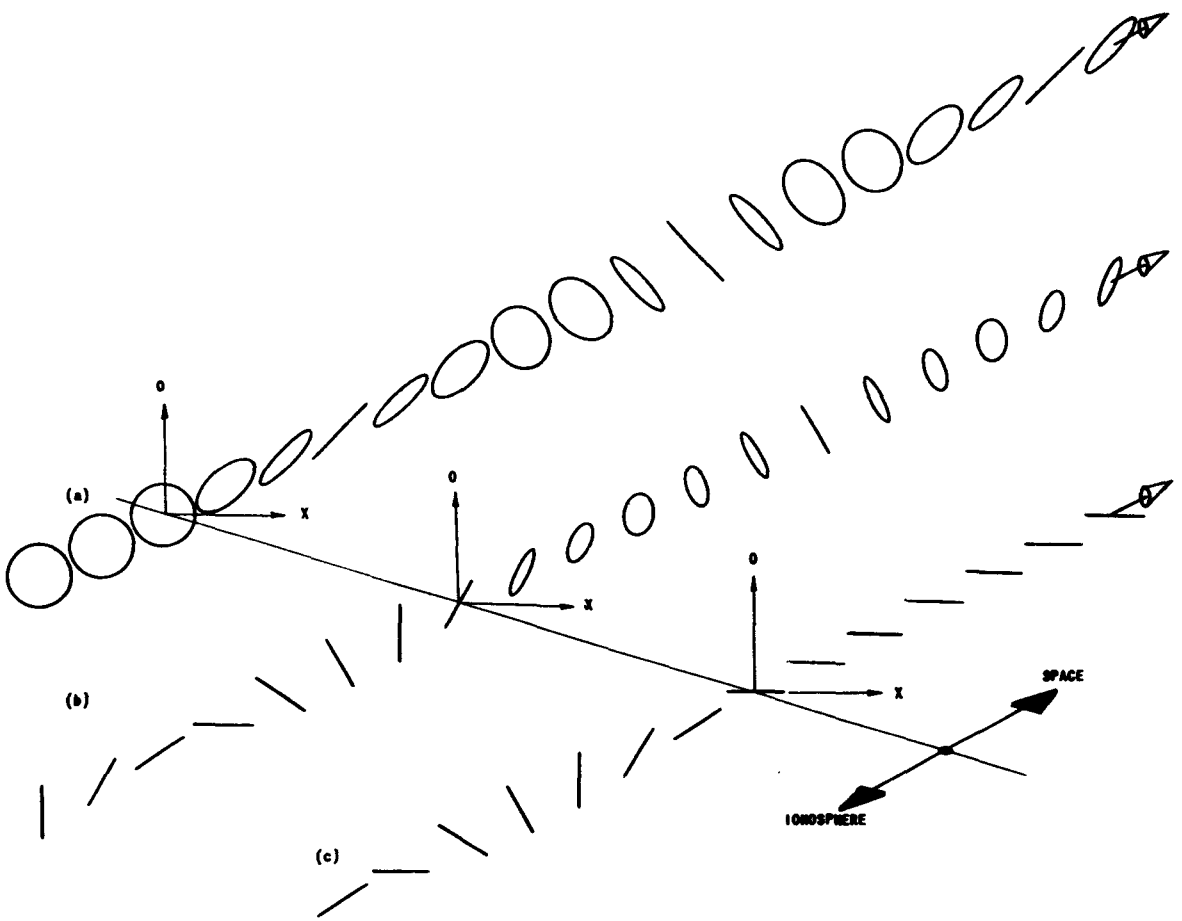

FIG. 5. POLARIZATION CHANGE OF EARTH-TRANSMITTED WAVE. "O" and "X" indicate the directions of ordinary and extraordinary waves in the particle stream. (a) Circular polarization is transmitted; (b) linear polarization is transmitted and excites some of each wave; (c) linear polarization is transmitted and excites only one wave.

D. MOON RADAR

A typical moon-radar experiment is illustrated in Fig. 6. A transmitter, T, sends a linearly polarized signal to the moon; the reflected signal is received on the transmitting antenna by receiver R_V. In passing out through the ionosphere the wave undergoes a Faraday rotation, ϕ_f. It then excites some of each characteristic wave in the particle stream. The "ordinary" wave lies at angle, ϕ_o, from the transmitted polarization. (The direction of this wave is perpendicular to the plane containing the ray path and the direction of particle flow. If particles are assumed to flow radially from the sun, the plane is that which includes the sun, moon, and earth.) The two waves propagate to the moon and back, changing their relative time phase by ϕ_p. Each then undergoes a second spatial rotation, ϕ_f, and finally reach the receiver.

The amplitude of the received signal, $|E_{RV}|$, is expressed below in terms of KE, the signal strength expected if there were no particles, and the three angles, ϕ_f, ϕ_p, and ϕ_o:

$$\frac{|E_{RV}|}{KE} = \frac{\sqrt{\cos^2 2\phi_o + \cos^2 2\phi_f + \cos\phi_p\,(\sin^2 2\phi_o - \sin^2 2\phi_f)}}{\sqrt{2}} \tag{25}$$

If a second antenna, linearly polarized perpendicular to the transmitting antenna, were used to receive the reflected signal, its amplitude, $|E_{RH}|$, would vary as,

$$\frac{|E_{RH}|}{KE} = \frac{\sqrt{\sin^2 2\phi_o + \sin^2 2\phi_f + \cos\phi_p\,(\cos^2 2\phi_o - \cos^2 2\phi_f)}}{\sqrt{2}} \tag{26}$$

Variations of these two quantities with the angles are shown in Fig. 7, $|E_{RV}|/KE$ by solid lines and $|E_{RH}|/KE$ by broken lines.

If the particle stream is absent or has a very low density, $\phi_p \approx 0°$, normal Faraday fading takes place for every 45° change in ϕ_f (a total of 90° for the two passages through the ionosphere). The depth of this fading is reduced and it can even be eliminated as stream densities (and ϕ_p) become large. When its densities are high and varying, the stream itself can cause fading, whose character depends on ϕ_o, the orientation of the antenna relative to the stream direction. Additional

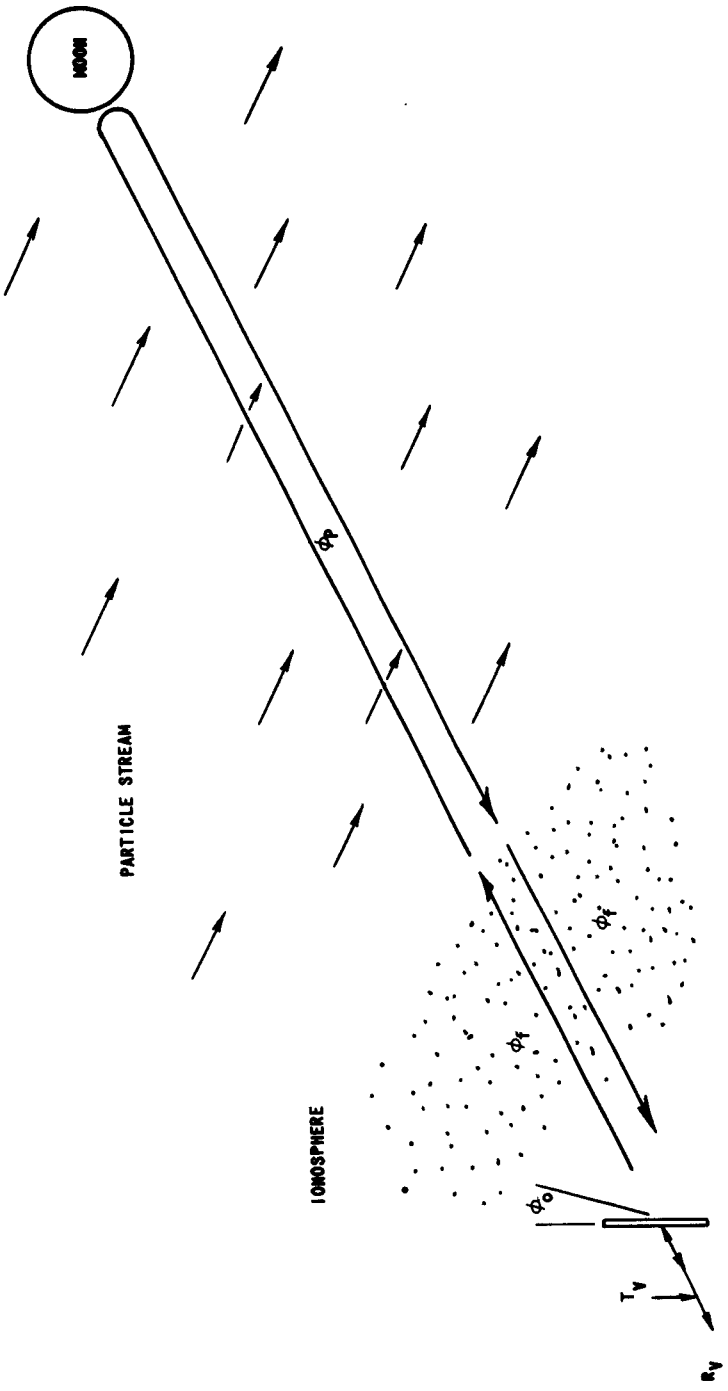

FIG. 6. MOON-RADAR EXPERIMENT.

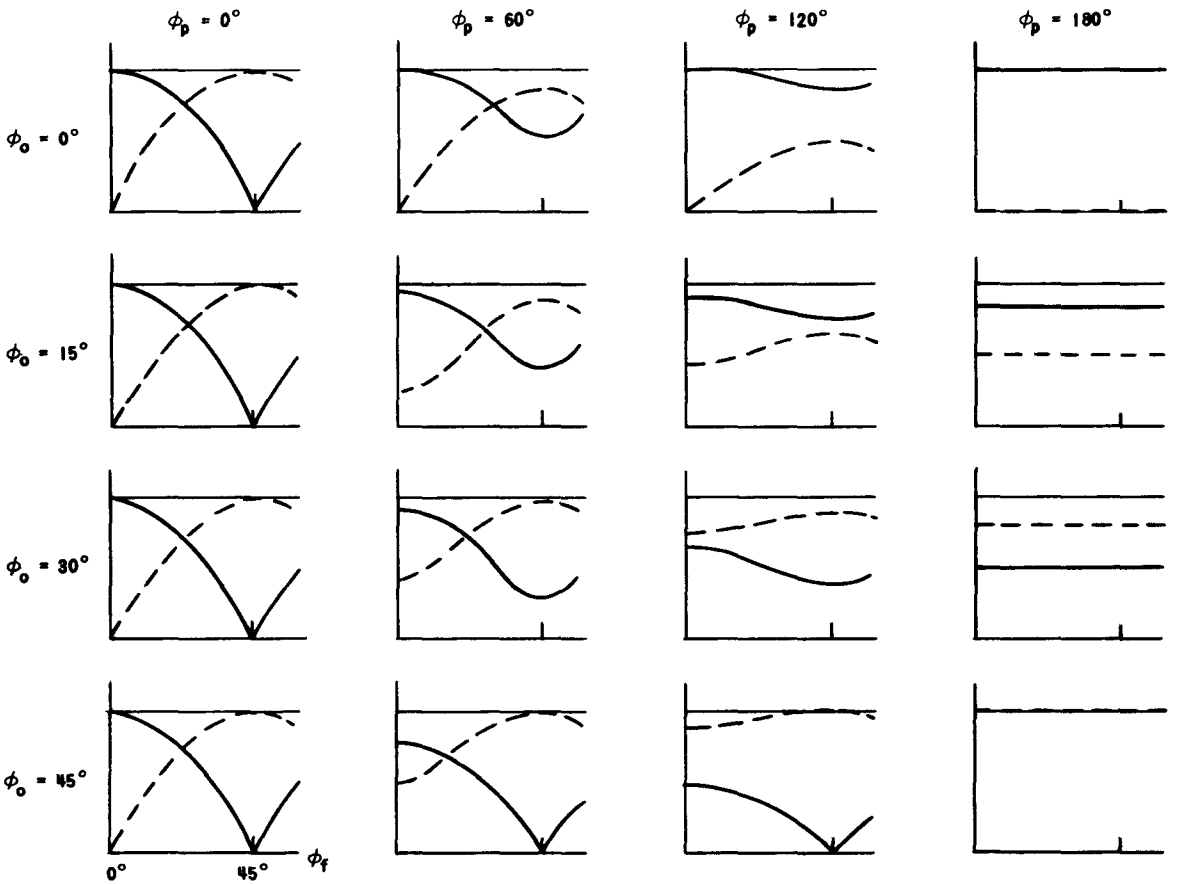

FIG. 7. SIGNAL STRENGTH VS POLARIZATION ANGLES. Signal strength of received vertical polarization, $|E_{RV}|$, is shown by solid lines, and of received horizontal polarization, $|E_{RH}|$, by broken lines; ϕ_f is the Faraday rotation angle and ϕ_o is the stream phase change.

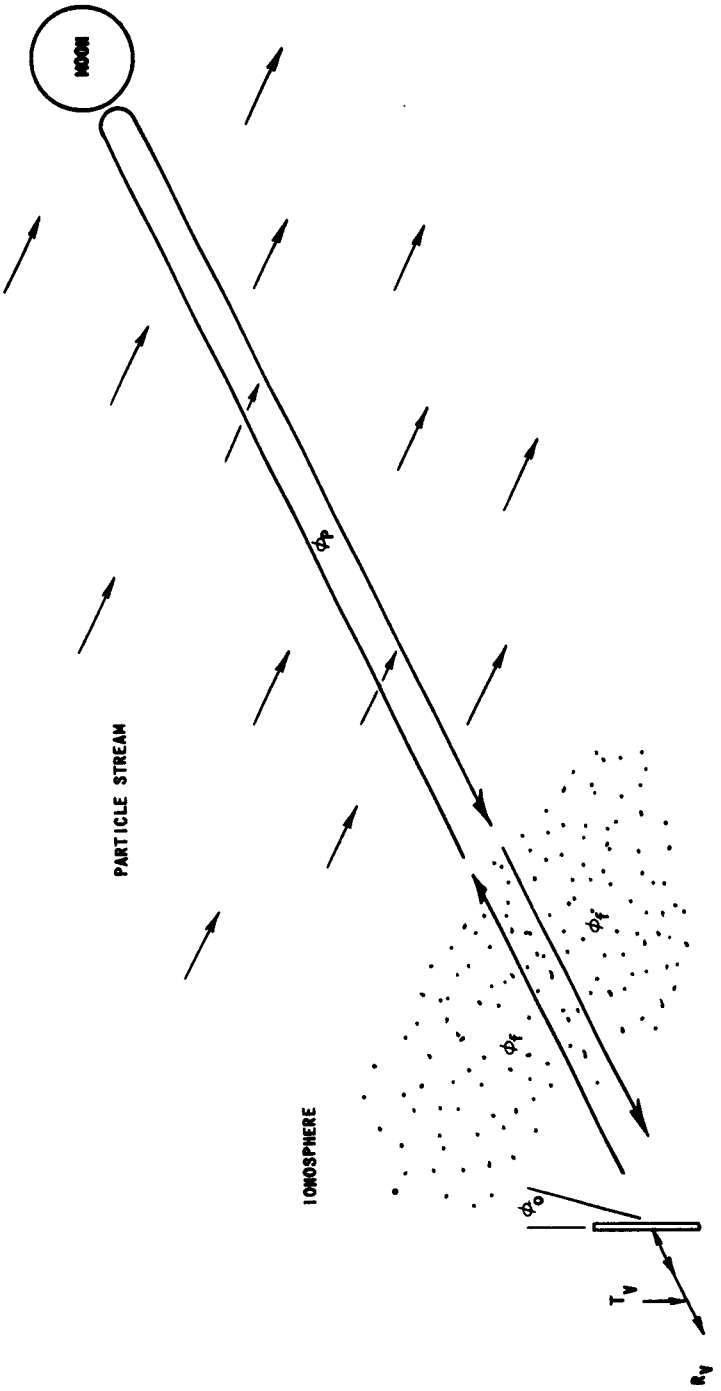

FIG. 6. MOON-RADAR EXPERIMENT.

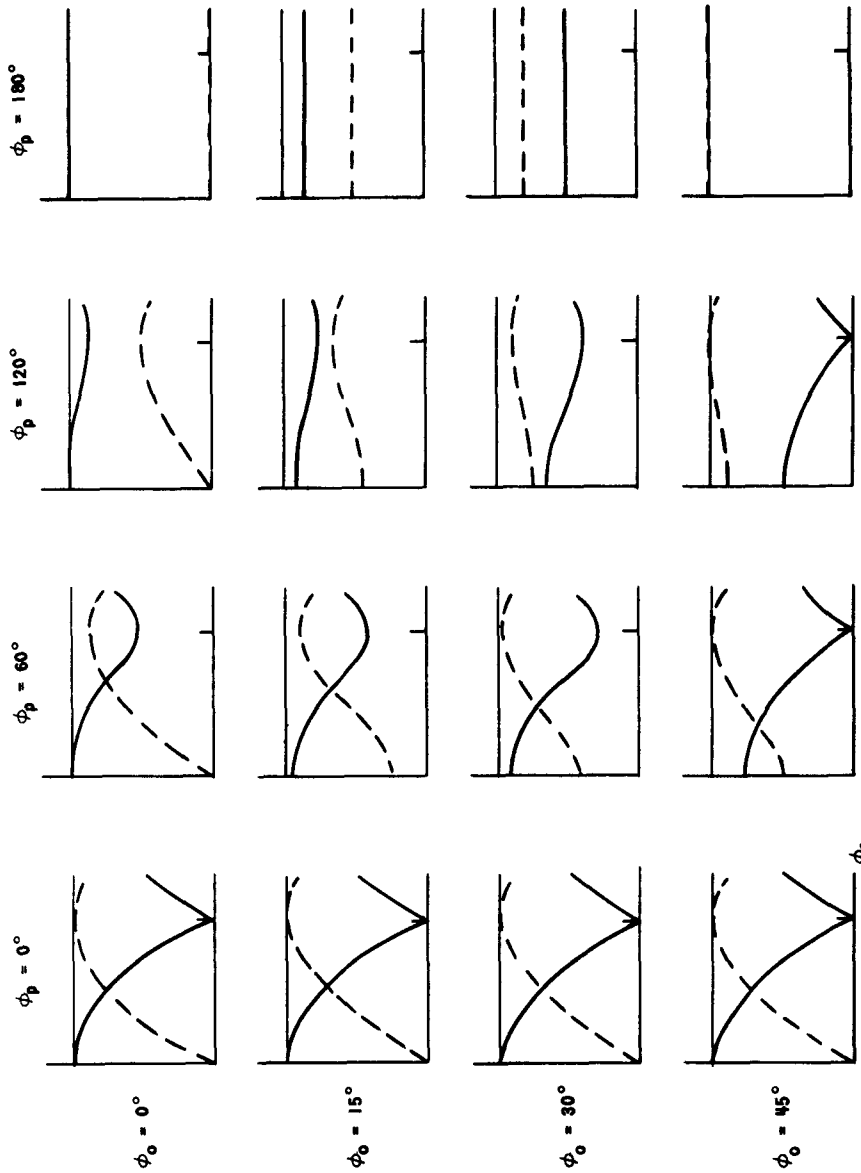

FIG. 7. SIGNAL STRENGTH VS POLARIZATION ANGLES. Signal strength of received vertical polarization, $|E_{RV}|$, is shown by solid lines, and of received horizontal polarization, $|E_{RH}|$, by broken lines; ϕ_f is the Faraday rotation angle and ϕ_o is the stream phase change.

variation of the received amplitudes may be caused by libration fading* introduced in the reflection from the moon. When these various fading effects take place simultaneously, quantitative interpretation of the data would be difficult and often impossible if only amplitude variations are recorded.

Moon-radar experiments can be designed to give clearer data on ϕ_f and ϕ_p; but before these are attempted, the presence of such particle stream effects should be verified by present moon-radar experiments, most of which are of the type just described. The most important evidence of a stream would be the presence of appreciable signal strength during expected Faraday nulls. While there are many phenomena that could cause extra variation in total signal strength, none has been suggested that can cause considerable depolarization of the wave. (Depolarization is necessary to prevent deep Faraday nulls when the received signal arrives rotated 90° from its transmitted linear polarization.) If such masking of Faraday nulls is observed, study of the time of its occurrence can further determine if particle streams are the cause. As the moon rotates about the earth, both ϕ_o (the angle between the antenna polarization and the normal to the earth-moon-sun plane) and Θ (the angle between the ray path and the stream direction) vary. These in turn cause changes in the effects of the particle streams. Thus, the effects should be smallest--best Faraday fading obtained--when Θ is near 90°, see Fig. 3. (This will occur near solar or lunar eclipse if the stream comes radially from the sun.) In addition good fading should be obtained when $\phi_o = \pm 45°$ for $|E_{RV}|$ or $\phi_o = 0°$ or 90° for $|E_{RH}|$, see Fig. 7. Under these conditions the Faraday rotation necessary to give the deep fade is also just right to excite only one characteristic wave in the stream, Fig. 5(c); therefore there is no depolarization.

If such investigations do indicate the presence of such particle streams, there are many moon-radar experiments which could be performed to acquire better data. One such experiment would be to transmit a

*The radar signals reflected from the edges of the moon combine in different phase with those from the center to cause fading. In addition, when the moon is librating (rocking on its axis), the edge signals are slightly doppler shifted and beat with the main part of the signal, thus causing a random low-frequency fluctuation in the amplitude of the reflected signal. It should be noted that while this effect can cause changes in the signal's amplitude, it cannot cause appreciable changes in its polarization characteristics and therefore could not reduce the depth of Faraday fading.

a circularly polarized wave and measure the polarization of the received wave. In this way equal amounts of the "O" and "X" waves are excited in outer space, Fig. 5(a). After undergoing relative phase shift, ϕ_p, the wave is elliptically polarized with the ratio of major to minor axis given by:

$$\frac{\text{major axis}}{\text{minor axis}} = \tan\left(\frac{\phi_p}{2} + 45^\circ\right) \quad \text{or} \quad \cot\left(\frac{\phi_p}{2} + 45^\circ\right) \tag{27}$$

Faraday rotation as the wave returns through the ionosphere does not change this ratio but merely rotates the entire ellipse by ϕ_f. Since the major axis of the ellipse will always be at $\pm 45^\circ$ from the "O" mode direction before reentering the ionosphere, the Faraday rotation is directly measured by the orientation of the received polarization ellipse relative to the earth-moon-sun plane (again assuming radial particle flow from the sun). As usual there is multiple rotation discrepancy in interpreting the angles measured, $\pm n\ 90^\circ$ in ϕ_f and $\pm n\ 45^\circ$ in ϕ_p. These discrepancies can be resolved either by keeping the frequency high (and rotations small) so that n can be estimated, or by making measurements at two different frequencies.

E. DEEP SPACE PROBE

A second experiment that would be affected by particle streams is one in which one or more transmitters send radio waves to a deep space probe. At the probe the received signal is analyzed and its characteristics are relayed back to earth via normal telementry channels. Such an experiment, presently being studied for use on future Venus and Mars vehicles, measures the phase path difference between two harmonically related signals to obtain the integrated electron density between earth and the vehicle. To avoid complications due to Faraday rotation in the ionosphere, these transmitters would send circularly polarized waves.

The experimental situation again is illustrated by the sketch in Fig. 5(a). The polarization ellipse of the signal received at the probe has a ratio of major to minor axis given by Eq. (27), where ϕ_p now is due to particle streams between the earth and the vehicle. The differences between this and the moon-radar experiment are:

1. There is only one passage through the ionosphere, eliminating all Faraday rotation effects if circular polarization is transmitted;
2. There is no reflection involved, thus eliminating a troublesome source of fading;
3. The streams affect the wave over a much greater distance (on the order of 1 AU), making the experiment sensitive to much lower densities;
4. The angle θ, between ray path and particle stream, will most likely vary over the path. (The directions of the "O" and "X" waves will not vary over the path since they are defined by the *normal* to the plane containing the ray path and the stream, the earth-probe-sun plane, assuming radial particle flow from the sun. Variations of θ along the path would be taken into account by integrating $\Delta(V,\theta)\ \hbar(V,\theta)$ along the path.)

The effects might also be detected by interplanetary radar experiments. However, at the frequencies normally used, near 2 kMc, the depolarization would be measurable only during high solar activity and its detection would be complicated both by poor signal-to-noise ratios and by surface depolarization during the reflection from the planet.

F. COSMIC RADIO SOURCES

A third measurement which would show particle stream effects is observation of cosmic radio sources. Recent observations have shown that a large number of such sources exhibit a net polarization, some as high as 15 percent [Ref. 7]. When radio waves from these sources pass close to the sun on their paths to the earth, the character of this net polarization will be changed if particle streams of sufficient density are present. An experiment then would consist of carefully measuring the character of polarization of a source when it is in a direction away from the sun and then looking for changes in this polarization as the ray path comes closer to the sun.

If particle streams flow radially from the sun and vary in density as $1/r^2$, where r is their distance from the sun, the total effective distance times effective particle density across the ray path varies approximately as

$$N_{eff} \times D_{eff} = N_o \frac{r_e^2}{r_{min}}$$

where N_o is the particle stream density at the earth, r_e is the earth's orbital radius, 1 AU, and r_{min} is the ray's closest approach

to the sun (assumed to be much less than r_e). For a minimum approach, r_{min}, equal to about 10 solar radii, r_e^2/r_{min} is approximately 2×10^9 km, 10 AU.

If the ray passes closer than about 10 solar radii, the neglect of the magnetic field and assumption of radial particle flow are most likely false and the theories derived here no longer apply. However, outside of the region affected by the solar corona the assumptions probably hold and the effects would be as described. The assumption of an even radial flow is probably also erroneous, a more accurate description being radial bursts of particles whose density varies in time and along the path. This would change the previous description only in that the effects would be integrated along the path, taking into account the density variation.

G. SENSITIVITIES OF THE EXPERIMENTS

The sensitivities of the three experiments depend on the frequencies, distance, and geometry, as well as the density and energy of the electron stream. These sensitivities are illustrated in Fig. 8, where the number of degrees depolarization due to the stream are shown for the three experiments. Values are shown for noisy and quiet solar conditions and for the expected range of electron velocities shown in Table 1. It is assumed that the angle between the ray and the particle stream is near optimum, 90^o for small β. The interation distances are assumed to be 7.4×10^5 km, 1 AU and 10 AU respectively for the moon radar, deep-space probe, and cosmic noise source.

From this it is apparent that if electrons and protons have equal velocity, only the deep-space-probe or cosmic-noise-source measurements will detect the stream and then only when it rises above its quiet values. But if protons and electrons are in energy equilibrium, all three experiments will detect the streams. The least sensitive experiment, moon radar, would have measurable effects only under slightly disturbed solar conditions, while the others would show appreciable effects even during quiet conditions. Note that even a 2-kMc telemetry signal in a space probe would be depolarized appreciably.

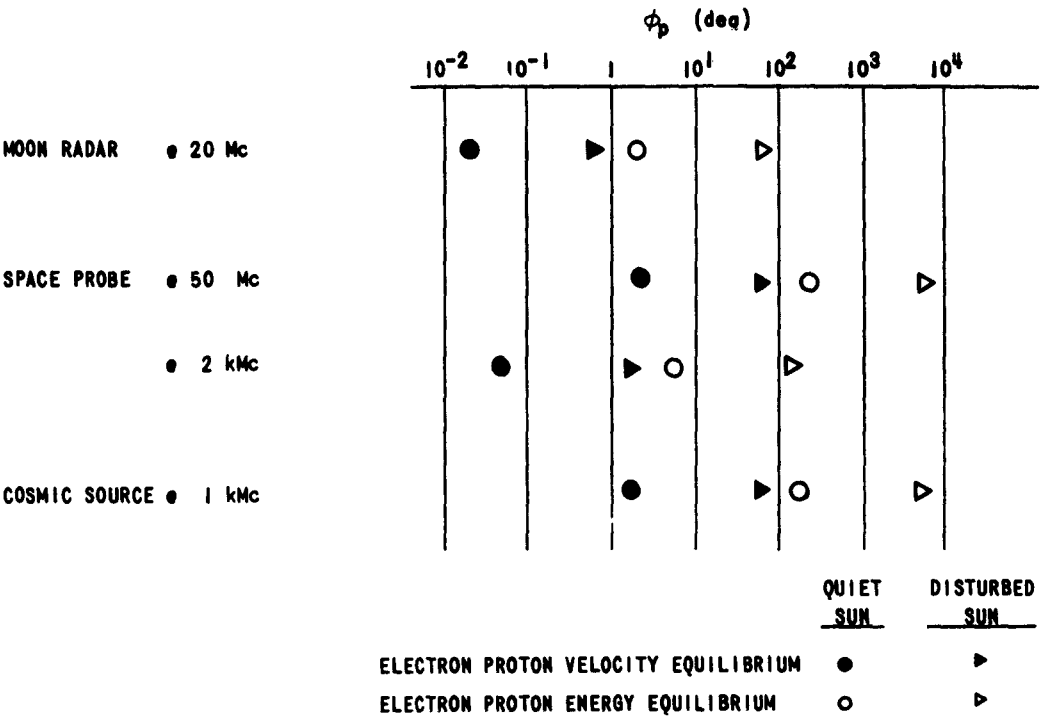

FIG. 8. SUMMARY OF EXPECTED DEPOLARIZATIONS. The depolarization angle, ϕ_p, is shown for various descriptions of the electron component of the solar wind as indicated.

IV. CONCLUSIONS

The above results show that the electron component of the solar wind, whose proton component has recently been measured by space vehicles, can be detected by the three suggested experiments. Although by themselves such experiments will not yield information on the spectrum of the electrons, simultaneous measurements of the proton component can give such information if approximate current neutrality is assumed. It should be noted that, although this discussion has dealt mostly with high but not relativistic velocities, electrons with $\beta \approx 0.6$ to 0.99 can have effects and need to be considered when interpreting results. In this energy range, stream densities as low as 3×10^{-2}, 3×10^{-4}, and 5×10^{-3} would affect the moon-radar, space-probe, and cosmic-noise-source results respectively.

In the moon-radar experiment, information on the wake of the earth's magnetosphere in the solar wind could also be obtained. In this region the normal streaming of the solar wind is made nearly random [Refs. 8 and 9] and it cannot depolarize radio waves. Therefore, by measuring the decrease in depolarization as the waves pass through it, the dimensions of the region might be deduced.

There are several avenues of interest suggested but not followed by the work presented here. For instance, a random particle velocity distribution is uninteresting for small particle densities but would give interesting results when the wave's phase velocity approached the particles' thermal velocity [see Eq. (14)]. Another interesting problem is the inclusion of an external magnetic field. Although the effects are negligible within the earth's magnetosphere for the frequencies used, they would not be negligible at lower frequencies or within the solar corona. Solutions of this complex problem could be applied to cosmic-noise-source measurements when the rays pass very close to the sun or possibly to measurements of auroral particle streams. In both of these measurements, it would probably be necessary to include particle collisions. Finally, although this report is concerned with geophysics and radio and radar astronomy, the results are applicable to beam-tube and hot-plasma research where high-velocity particles are also encountered.

APPENDIX A. RELATIVISTIC MASS VARIATION

The instantaneous mass of a particle moving in a fixed coordinate system is given by

$$m = \frac{m_o}{\sqrt{1 - \frac{v^2}{c^2}}}$$

where m_o is the rest mass of the particle, c is the velocity of light, and v is the magnitude of the particle's total velocity in the referenc (fixed frame) coordinates. In the derivation v^2 is given by

$$v^2 = (V_x + v_x)^2 + (V_y + v_y)^2 + (V_z + v_z)^2$$

$$= V_x^2 + V_y^2 + V_z^2 + 2(V_x v_x + V_y v_y + V_z v_z) + v_x^2 + v_y^2 + v_z^2$$

$$= V^2 + 2(V_x v_x + V_y v_y + V_z v_z)$$

where $V^2 = V_x^2 + V_y^2 + V_z^2$. The inequality $v_i << V_i$ has been used. Substituting this result into the mass equation,

$$m = \frac{m_o}{\sqrt{1 - \frac{V^2}{c^2} - \frac{2(V_x v_x + V_y v_y + V_z v_z)}{c^2}}}$$

$$m = \frac{m_o}{\sqrt{1 - \frac{V^2}{c^2}}} \frac{1}{\sqrt{1 - \frac{2(V_x v_x + V_y v_y + V_z v_z)}{(1 - V^2/c^2)c^2}}} \tag{29}$$

Since the term involving $V_x v_x$, etc., is $<< 1$ ($v << V < c$), the radical can be replaced as shown below:

$$m = \frac{m_o}{\sqrt{1 - V^2/c^2}} \left[1 + \frac{1}{2} \times 2 \times \frac{(V_x v_x + V_y v_y + V_z v_z)}{(1 - V^2/c^2)c^2} \right] \tag{30}$$

This can be expressed as

$$m = m_o \gamma \, [1 + d]$$

where γ and d are as defined in Eq. (4).

The step from (29) to (30) is invalid if $(1 - V^2/c^2)$ approaches v/c, the perturbation velocity over the speed of light. For radio-wave field strengths of 1 v/cm at 20 Mc, this limit is approached when $(1 - V^2/c^2) = 2 \times 10^{-7}$, i.e., $\beta = 0.9999998$. Particles of this and higher velocities have such high relativistic masses that their effect on the wave would be completely negligible.

APPENDIX B. DOPPLER-SHIFT EFFECT

The field seen by the moving particle varies as $\sin(\omega t - \Gamma X_p)$, where $X_p = \int v_x dt$ is the instantaneous position of the particle. Assuming v_x to be given by

$$v_x = V_x + v_x \sin \omega t$$

$$X_p = V_x t - \left(\frac{v_x}{\omega}\right) \cos \omega t$$

The field thus varies as

$$\sin \left[\omega t - \Gamma V_x t + \left(v_x \frac{\Gamma}{\omega}\right) \cos \omega t\right]$$

The derivative of this function gives

$$\left\{ \cos\left[\omega t - \Gamma V_x t + \left(v_x \frac{\Gamma}{\omega}\right) \cos \omega t\right] \right\} \left(\omega - \Gamma V_x - \Gamma v_x \sin \omega t \right)$$

The term $\Gamma v_x \sin \omega t$ can be dropped since its magnitude is much smaller than ΓV_x, $v \ll V$. Thus the derivative has the form

$$\omega \left(1 - \frac{\Gamma V_x}{\omega}\right) \cos (\omega t - \Gamma X_p)$$

In the exponential form this is equivalent to time derivatives generating factors $j\omega(1 - \Gamma V_x/\omega)$.

These results are invalid if $(1 - \Gamma V_x/\omega)$ approaches v/c. But once again this corresponds to particles with very high relativistic masses whose contribution to the wave interaction is negligible.

REFERENCES

1. M. Neugubauer and C. W. Snyder, "The Mission of Mariner II; Preliminary Observations, Solar Plasma Experiment," *Science, 138*, 7 Dec 1962, pp. 1095-1100.
2. K. I. Gringauz, et al, "A Study of the Interplanetary Ionized Gas, High-Energy Electrons, and Corpuscular Radiation from the Sun by Means of the Three-Electrode Trap for Charged Particles on the Second Soviet Cosmic Rocket," *Soviet Phys. Doklady, 5*, 1960, p. 361. (Translated from *Doklady Akad. Nauk SSSR, 131*, 6, April 1960, pp. 1301-1304.)
3. W. G. V. Rosser, et al, "Electrons in the Earth's Outer Radiation Zone," *J. Geophys. Res., 67*, 12, Nov 1962, pp. 4533-4542.
4. R. L. Smith, "Properties of the Outer Ionosphere Deduced from Nose Whistlers," *J. Geophys. Res., 66*, 11, Nov 1961, pp. 3709-3716.
5. H. B. Liemohn and F. L. Scarf, "Whistler Attenuation by Electrons with an $E^{-2.5}$ Distribution," *J. Geophys. Res., 67*, 11, Oct 1962, pp. 4163-4167.
6. J. V. Evans, "The Electron Content of the Ionosphere," *J. Atmos. and Terr. Phys., 11*, 1957, pp. 259-271.
7. L. Woltjer, "The Polarization of Radio Sources," *Astrophys. J., 136*, 3, Nov 1962, pp. 1152-1154.
8. W. I. Axford, "The Interaction between the Solar Wind and the Earth's Magnetosphere," *J. Geophys. Res., 67*, 10, Sep 1962, pp. 3791-3796.
9. P. J. Kellog, "Flow of Plasma around the Earth," *J. Geophys. Res., 67*, 10, Sep 1962, pp. 3805-3811.

DISTRIBUTION LIST FOR

AFCRL-62-1122 SEL-63-041

1 Science Advisor
Department of State
Washington 25, D.C.

1 Office of Secretary of Defense
(DDR and E) Tech. Library
Washington 25, D.C.

1 Institute of Technology Library
MCLI-LIB, Bldg. 125, Area B
Wright-Patterson Air Force Base,
Ohio

1 Hq. USAF (AFCSA) Secretary
Washington 25, D.C.

20 AFCRL, OAR (CRXRA) Stop 39
L.G. Hanscom Field
Bedford, Mass.

1 ARL (ARA-2)
Library AFL 2292, Bldg. 450
Wright-Patterson AFB, Ohio

1 ESD (ESRDG)
L.G. Hanscom Field
Bedford, Mass.

1 ASD (ASAPRD-Dist)
Wright-Patterson AFB, Ohio

1 ACIC (ACDEL-7)
2d and Arsenal
St. Louis 18, Mo.

1 NAFEC Library Branch, Bldg. 3
Atlantic City, N.J.
Attn: RD-702

1 AFCRL, OAR (CRXR, John R. Marple)
L.G. Hanscom Field
Bedford, Mass.

1 AWS (AWSSS/SIPD)
Scott AFB, Ill.

1 A. U. (Library)
Maxwell AFB, Ala.

1 Office of the Chief of R and D
Department of the Army
The Pentagon, Wash. 25, D.C.

1 Technical Documents Center
Evans Signal Labs.
Belmar, N.J.

1 Army Research Office
Environmental Research Division
3045 Columbia Pike
Arlington 4, Va.

1 Commanding Officer
U.S. Army Electronic R and D Lab.
Fort Monmouth, N.J.
Attn: ERDA/SL/SMA

1 Technical Reports Librarian
U.S. Naval Postgraduate School
Monterey, Calif.

1 Director
U.S. Naval Research Laboratory
Code 2027
Washington 25, D.C.

1 ONR (Geophysics Code N-416)
Office of Naval Research
Washington 25, D.C.

1 Documents Expediting Project
(UNIT X)
Library of Congress
Washington 25, D.C.

1 Superintendent of Documents
Government Printing Office
Washington 25, D.C.

1 National Research Council
2101 Constitution Ave.
Washington 25, D.C.

1 NASA
Attn: Library, Code AFET-LA
Stop 85
Washington 25, D.C.

1 Librarian
Boulder Laboratories
National Bureau of Standards
Boulder, Colorado

1 Library
National Bureau of Standards
Washington 25, D.C.

1 Director of Meteorological Res.
U.S. Weather Bureau
Washington 25, D.C.

1 Library
U.S. Weather Bureau
Suitland, Md.

20 ASTIA (TIPAA)
Arlington Hall Station
Arlington 12, Va.

1 Director, USAF Project RAND
The Rand Corporation
1700 Main St.
Santa Monica, Calif.
Thru: A.F. Liaison Office

1 Dr. William W. Kellogg
Rand Corporation
1700 Main St.
Santa Monica, Calif.

1 Mr. Malcolm Rigby
American Meteorological Society
P.O. Box 1736
Washington 13, D.C.

1 Inst. of Aerospace Sciences, Inc.
2 East 64th St.
New York 21, N.Y.

1 Library
Geophysical Institute
University of Alaska
P.O. Box 938
College, Alaska

1 Dr. Joseph Kaplan
Dept. of Physics
University of California
Los Angeles, Calif.

1 Prof. Fred L. Whipple
Harvard College Observatory
60 Garden St.
Cambridge 38, Mass.

1 Dr. David Fultz
Dept. of Geophysical Sciences
University of Chicago
Chicago 37, Ill.

1 Dr. A.M. Peterson
Stanford University
Stanford, Calif.

1 Prof. Clarence Palmer
Institute of Geophysics
University of California
Los Angeles 24, Calif.

1 Technical Information Office
European Office, Aerospace Res.
Shell Building, 47 Cantersteen
Brussels, Belgium

2 Defence Research Member
Canadian Joint Staff
2450 Massachusetts Ave., N.W.
Washington 8, D.C.

1 Hq. USAF (AFRDR)
Washington 25, D.C.

Stanford Electronics Laboratory, Stanford University, Stanford, Calif. Rept. No. SEL-63-041. DETECTION OF SOLAR PARTICLE STREAMS USING HIGH-FREQUENCY RADIO WAVES by Bruce B. Lusignan. Apr 63, 34 pp. incl. 8 illus., 1 table, 9 refs. (TR No. 1403-3, AFCRL-62-1122) Unclassified Report.

It is shown that streams of high-velocity, low-density charged particles in the absence of any external magnetic field make a medium anisotropic to radio waves. Such a medium will propagate two waves of unchanging (characteristic) polarization, one linearly polarized perpendicular to the stream and the second at right angles to the first.

Such streams are present in the electron component of the solar wind. Three experiments – moon radar, transmission to a space probe, and observation of polarized cosmic sources – are proposed as a means of measuring these solar streams.

1. Radio Propagation
2. Plasma Physics
3. Radio Astronomy
4. Solar Particles

I. AFSC Project 7661, Task 76615
II. Contract AF19(604)-7994
III. Geophysics Research Dir, AFCRL, Office of Aerospace Research, Bedford, Mass.
IV. Not aval fr OTS
V. In ASTIA collection

Stanford Electronics Laboratory, Stanford University, Stanford, Calif. Rept. No. SEL-63-041. DETECTION OF SOLAR PARTICLE STREAMS USING HIGH-FREQUENCY RADIO WAVES by Bruce B. Lusignan. Apr 63, 34 pp. incl. 8 illus., 1 table, 9 refs. (TR No. 1403-3, AFCRL-62-1122) Unclassified Report.

It is shown that streams of high-velocity, low-density charged particles in the absence of any external magnetic field make a medium anisotropic to radio waves. Such a medium will propagate two waves of unchanging (characteristic) polarization, one linearly polarized perpendicular to the stream and the second at right angles to the first.

Such streams are present in the electron component of the solar wind. Three experiments – moon radar, transmission to a space probe, and observation of polarized cosmic sources – are proposed as a means of measuring these solar streams.

1. Radio Propagation
2. Plasma Physics
3. Radio Astronomy
4. Solar Particles

I. AFSC Project 7661, Task 76615
II. Contract AF19(604)-7994
III. Geophysics Research Dir, AFCRL, Office of Aerospace Research, Bedford, Mass.
IV. Not aval fr OTS
V. In ASTIA collection

Stanford Electronics Laboratory, Stanford University, Stanford, Calif. Rept. No. SEL-63-041. DETECTION OF SOLAR PARTICLE STREAMS USING HIGH-FREQUENCY RADIO WAVES by Bruce B. Lusignan. Apr 63, 34 pp. incl. 8 illus., 1 table, 9 refs. (TR No. 1403-3, AFCRL-62-1122) Unclassified Report.

It is shown that streams of high-velocity, low-density charged particles in the absence of any external magnetic field make a medium anisotropic to radio waves. Such a medium will propagate two waves of unchanging (characteristic) polarization, one linearly polarized perpendicular to the stream and the second at right angles to the first.

Such streams are present in the electron component of the solar wind. Three experiments – moon radar, transmission to a space probe, and observation of polarized cosmic sources – are proposed as a means of measuring these solar streams.

1. Radio Propagation
2. Plasma Physics
3. Radio Astronomy
4. Solar Particles

I. AFSC Project 7661, Task 76615
II. Contract AF19(604)-7994
III. Geophysics Research Dir, AFCRL, Office of Aerospace Research, Bedford, Mass.
IV. Not aval fr OTS
V. In ASTIA collection

Stanford Electronics Laboratory, Stanford University, Stanford, Calif. Rept. No. SEL-63-041. DETECTION OF SOLAR PARTICLE STREAMS USING HIGH-FREQUENCY RADIO WAVES by Bruce B. Lusignan. Apr 63, 34 pp. incl. 8 illus., 1 table, 9 refs. (TR No. 1403-3, AFCRL-62-1122) Unclassified Report.

It is shown that streams of high-velocity, low-density charged particles in the absence of any external magnetic field make a medium anisotropic to radio waves. Such a medium will propagate two waves of unchanging (characteristic) polarization, one linearly polarized perpendicular to the stream and the second at right angles to the first.

Such streams are present in the electron component of the solar wind. Three experiments – moon radar, transmission to a space probe, and observation of polarized cosmic sources – are proposed as a means of measuring these solar streams.

1. Radio Propagation
2. Plasma Physics
3. Radio Astronomy
4. Solar Particles

I. AFSC Project 7661, Task 76615
II. Contract AF19(604)-7994
III. Geophysics Research Dir, AFCRL, Office of Aerospace Research, Bedford, Mass.
IV. Not aval fr OTS
V. In ASTIA collection